THE UNIVERSITY OF MICHIGAN

INDUSTRY PROGRAM OF THE COLLEGE OF ENGINEERING

THE EFFECTS OF ULTRASONIC ENERGY UPON EVAPORATION OF FUEL DROPS

William Mirsky
Assistant Professor of Mechanical Engineering

Jay A. Bolt
Professor of Mechanical Engineering

April, 1958

IP-284

INTRODUCTION

A more complete understanding of the factors involved in the combustion of liquid fuels, and possible means for increasing their rate of combustion, remain important objectives.

Because of the extremely complex nature of evaporation and combustion processes for liquid drops and the difficulties involved in measurements, most investigators have chosen to study the evaporation or burning processes associated with an isolated drop. Many of these researches have employed fine filaments to hold the drops in space while observations are made.

Studies were made at the University of Michigan to establish means for holding liquid drops in space without any attachments[1]. Attempts were first made to stabilize a drop on a rising air stream. This proved impractical, and an ultrasonic field was added to give transverse stability. The combination of air drag force and ultrasonic field made it possible to hold a drop fixed in space while evaporation occurred.

As would be expected, tests revealed that the ultrasonic energy affected the rates of evaporation and combustion, and it therefore became necessary to evaluate these rates with and without the ultrasonic energy. In the course of determining the evaporation rate without ultrasonic energy a new expression for drop evaporation was developed.

Cumene was used for the greater part of this study because of its suitable rate of evaporation and relatively low cost for the pure grade of fuel used.

EXPERIMENTAL EQUIPMENT

The experimental equipment is shown schematically in Figure 1. This equipment comprises four functional systems, as follows:

1. Air-flow system
2. Ultrasonic field generating system
3. Photographic recording system
4. Instrumentation and accessories

The air flow system provides a stream of low turbulence air flowing upward through a crystal cylinder of barium titanate. This cylinder is 4" long and 1-5/8" inside diameter. This ceramic piezo-electric transducer produces a concentric standing wave ultrasonic field in the air within the tube. The ultrasonic field, when stationary, i.e., when the wave nodes are fixed, introduces lateral forces on the drop within the tube which holds the drop in a fixed horizontal position. At the same time, the action of the rising air stream on the drop creates an upward drag force which can balance the downward force of gravity. By control of the air velocity and ultrasonic field, a drop may thus be held stationary in space. Motion pictures of the drop were taken at known time intervals to obtain drop diameter as a function of time.

Efforts were made to burn drops with this equipment by using a heated air stream. This introduced difficulties due to change in the velocity of sound in the air and shift in the resonant frequency. Further, to protect the crystal from overheating, it was provided with a coolant jacket, but this substantially reduced the ultrasonic energy transmitted.

RESULTS

Experimental data for evaporating drops were obtained from silhouette photographs taken with a 16-mm motion picture camera. In one series of tests the drops were suspended on fine glass filaments, approximately sixty microns in diameter, in constant velocity air streams. Tests were made at several relative

air velocities and sound field intensities. The second series of tests was made with free drops at their terminal velocity in a moving air stream. The drops were actually maintained at a fixed position in space by the combined effects of air drag and ultrasonic forces. Typical sequence photographs for both tests are shown in Figures 2 and 3. The greater reduction in size and reduced drop-shape distortion is evident with free drops.

EVAPORATION OF DROPS WITHOUT ULTRASONIC ENERGY, DROPS ON FILAMENTS

In an attempt to describe the experimental evaporation data obtained for drops on filaments by the widely accepted equation obtained by Godsave[2],

$$D^2 = D_o^2 - \lambda_1 t, \qquad (1)$$

the data from twenty-four tests at various relative air velocities were plotted showing D^2 as a function of t. The resulting curves were not straight lines as expected but showed some degree of curvature, the curvature increasing with an increase in relative air velocity. Using measurements from curves giving D as a function of t, it was possible to compute the exponent n to which the diameter had to be raised to make D^n a linear function of t. The evaporation process could then be closely approximated by the equation

$$D^n = D_o^n - \lambda t \qquad (2)$$

where n was found to be a function of relative air velocity as shown in Figure 4. The exponent appears to approach the value 2.0 at zero velocity so that Equation (1) becomes a limiting case of Equation (2).

A mathematical analysis of the evaporation process for constant relative air velocity, based on heat transfer to the drop through a spherically symmetric boundary layer led to quite a different result than presented by Equation (2). The introduction of boundary layer equations developed by Tomotika[3] into the equations for heat transfer led to the following evaporation equation:

$$\Delta D^{3/2} - \frac{3C}{2}\Delta D + 3C^2\,\Delta D^{1/2} - 3C^3\,\ell n\left\{\frac{D_o^{1/2}+C}{D^{1/2}+C}\right\} = \frac{6k}{C\rho c}\ell n\left\{1 + \frac{c(T_f-T)}{L}\right\}t \quad (3)$$

where

$$\Delta D^n = (D_o^n - D^n) \quad \text{and} \quad C = \frac{2}{f(N_{Pr})^{1/3}(\frac{v}{v})^{1/2}} \quad . \qquad (3a)$$

The development is presented in the Appendix. In the analysis, if the assumption is made that the ratio D/D_f remains constant during the entire evaporation process the result reduces to Equation (1).

The results of the analysis can also be expressed in terms of an expression for the Nusselt number

$$N_{Nu} = \alpha[2 + f\ (N_{Pr})^{1/3}\ (N_{Re})^{1/2}] \qquad (4)$$

which is similar to the results obtained by several other investigators[4,5,6,7]. The experimental data of this investigation are well correlated by this expression as shown in Figure 5.

The factor f in Equations (3a) and (4) is a semi-empirical factor which was assumed to vary only with relative velocity. It arises from the analysis of the assumed simplified boundary layer and would be difficult to define accurately in terms of more fundamental properties of the actual physical system.

Good agreement between theory, as represented by Equation (3), and experiment is indicated in Figure 6. The factor f was evaluated at one point on the evaporation curve (D = 600 microns) for each relative air velocity. These values were then used in Equation (3) to predict drop size during evaporation.

EVAPORATION OF DROPS WITH ULTRASONIC ENERGY

a) Drops on Filaments

Approximately eighty tests were made with evaporating drops on filaments in the presence of an ultrasonic field. Equation (2) was used to compare the evaporation rates obtained from these tests with those obtained with no ultrasonic field. It was found that the field had a pronounced effect on evaporation, especially at low relative air velocities where a maximum increase in the evaporation constant of 58 per cent was obtained. The results of these tests are summarized in Figure 7.

The peculiar rise and fall of the curves at low voltages is believed to be a characteristic of the ultrasonic field generating system, representing an initial rise and then fall of field intensity with an iincrease in voltage applied across the barium titanate transducer.

Evaporation rates were found to be extremely sensitive to slight changes in some of the ultrasonic system variables, especially with regard to the location of the drop in relation to the stationary nodes of the ultrasonic field and to variations in the frequency applied to the transducer. Maximum effects on evaporation were obtained with the drops located in the nodes and with the transducer operating at its resonant frequency of approximately 35,000 cycles per second.

b) Free Drops

A limited number of tests were made with freely suspended drops as illustrated in Figure 3. These tests also indicated an increase in evaporation rate with an increase in ultrasonic energy but experimental difficulties and lack of control of some of the variables in the sound generating system precluded any accurate measurements of evaporation rates.

CONCLUDING REMARKS

To evaluate the effects of ultrasonic energy on drop evaporation, it was first necessary to obtain evaporation data without this energy. The resulting experimental data were not described well by Equation (1) so new evaporation equations were developed. Equation (2) is entirely empirical while Equation (3) was derived by considering the heat transfer and boundary layer equations for a simplified drop model. Both Equations (2) and (3) adequately defined the experimental rate of evaporation.

When $D_o^{1/2} < C$, which is the case for very small drops ($D_o <$ 100 microns approx.) at very low velocities ($v <$ 1 fps approx.), Equation (3) reduces to

$$\Delta D^2 + \sum_{n=1}^{\infty} (-1)^n \frac{4}{(4+n)C} \Delta D^{\left(\frac{4+n}{2}\right)} = \frac{8k}{\rho c} \ell n \left(1 + \frac{c\Delta T}{L}\right)t. \qquad (5)$$

For relative air velocity approaching zero, the equation is approximated by

$$D_o^2 - D^2 = \frac{8k}{\rho c} \ell n \left(1 + \frac{c\Delta T}{L}\right)t \qquad (6)$$

which is similar to Equation (1).

With the introduction of ultrasonic energy in the form of standing waves, an increase in evaporation rate was obtained. The field appears to be effective in decreasing the boundary layer thickness by molecular agitation, thereby increasing heat and mass transfer rates through increased thermal and concentration gradients. A similar condition is brought about by an increase in relative air velocity. The investigation shows that the effectiveness of the ultrasonic energy for increasing evaporation rates is reduced as the relative velocity increases.

The experimental apparatus proved quite interesting in its ability to hold drops relatively motionless in space for long periods of time. One drop of kerosene was freely suspended for approximately two hours before the test was

stopped. Visual inspection of the drop with a small pocket microscope clearly indicated the internal liquid circulation.

Preliminary tests have been conducted with single burning drops in an ultrasonic field. An increase in the color intensity of the flame and a decrease in smokiness was noted in the presence of the field. However, the experimental difficulties mount rapidly when working with burning drops.

A preliminary set-up has also been made whereby a burning spray has been subjected to a high frequency electrostatic field produced between two plates. Visual observations and photography reveal that this energy also has an influence on combustion, which is made evident by shorter flames and reduction in smoke.

SYMBOLS

A_r	surface area of sphere having radius r
C_1	constant
C	$2/f\ (N_{Pr})^{1/3}(\frac{v}{\nu})^{1/2}$
D	diameter of drop
D_f	diameter of outer surface of equivalent thermal boundary layer
D_o	initial drop diameter
h	film heat transfer coefficient
L	latent heat of liquid drop
M	mass of drop
T	temperature of drop surface
T_f	temperature at outer surface of thermal boundary layer
T_r	temperature at surface of sphere having radius r
V	volume of drop
c	specific heat of vapor at constant pressure
f	$3 \sin \Theta/2C_1f_1$
f_1	proportionality constant
k	thermal conductivity
n	exponent in evaporation equation
n	integer
r	radius
t	time
v	relative air velocity
v_1	relative air velocity at outer surface of dynamic boundary layer
δ	thickness of dynamic boundary layer
δ_t	thickness of simplified thermal boundary layer

SYMBOLS (Cont'd)

θ angle at center of drop measured from forward stagnation point

λ empirical evaporation constant

λ_1 evaporation constant due to Godsave

μ absolute viscosity

ν kinematic viscosity

ρ density of liquid drop

$N_{Nu} = \frac{hD}{k}$ = Nusselt number

$N_{Pr} = \frac{c\mu}{k}$ = Prandtl number

$N_{Re} = \frac{Dv}{\nu}$ = Reynolds number

ACKNOWLEDGMENTS

The authors are grateful to the Power Plant Laboratory, Wright Air Development Center, for making the experimental part of this study possible through projects with the Engineering Research Institute of the University of Michigan. Continuing research in the field of combustion is presently being sponsored by the Office of Scientific Research of the United States Air Force.

REFERENCES

1. Mirsky, William, "The Evaporation of Single Liquid Drops, Including the the Effects of Ultrasonic Energy on Evaporation," Ph.D. Thesis, University of Michigan, 1956.

2. Godsave, G. A. E., "Studies of the Combustion of Drops in a Fuel Spray--The Burning of Single Drops of Fuel," Fourth Symposium (International) on Combustion, Baltimore, The Williams and Wilkins Company, 1953.

3. Tomotika, S., "The Laminar Boundary Layer on the Surface of a Sphere in a Uniform Stream," Reports and Memoranda No. 1678, Technical Report of the Aeronautical Research Committee (England), July, 1935.

4. Frossling, N., "Uber die Verdunstung fallender Tropfen," Gerlands Beitrage d. Geophysik, 52, 170 (1938).

5. Kinzer, G. D., and Gunn, R., "The Evaporation, Temperature and Thermal Relaxation-Time of Freely-Falling Waterdrops," Journal of Meteorology, 8, 71 (1951).

6. Ingebo, R. D., Vaporization Rates and Heat-Transfer Coefficients for Pure Liquid Drops, NACA TN-2368 (1951).

7. Ranz, W. E., and Marshall, W. R., "Evaporation from Drops, Part I," Chem. Eng. Prog., 48, 141 (1952); Part II, ibid., p. 173.

APPENDIX

Figure 8 illustrates the assumed model of the spherically symmetric evaporating drop. The equivalent isothermal surface with diameter D_f represents the outer edge of the assumed spherical boundary layer. Equating the rate of heat transfer through the boundary layer to the rate of enthalpy rise of the liquid as it is evaporated at the drop surface and heated as vapor in the boundary layer,

$$-k\, A_r \left(\frac{dT}{dr}\right)_r = [L + c(T_r - T)] \frac{dM}{dt}\,, \tag{7}$$

and integrating between proper limits on r and T gives

$$\frac{dM}{dt} = -\frac{\pi k D}{c} \left(\frac{2}{1-D/D_f}\right) \ell n \left[1 + \frac{c(T_f-T)}{L}\right]\,. \tag{8}$$

The mass rate of evaporation can also be expressed by

$$\frac{dM}{dt} = \frac{d}{dt}(\rho V) = \frac{\pi \rho D^2}{2} \frac{dD}{dt}\,. \tag{9}$$

Equating expressions for $\frac{dM}{dt}$, integrating between proper limits on D and t, and letting $(T_f-T) = \Delta T$,

$$D^2 - D_o^2 - 2 \int_{D_o}^{D} \left(\frac{D^2}{D_f}\right) dD = -\frac{8k}{\rho c} \ell n \left(1 + \frac{c\Delta T}{L}\right) t. \tag{10}$$

A complete solution requires a knowledge of the functional dependence of D_f upon D.

If D/D_f is assumed constant, further integration yields

$$D^2 - D_o^2 = -\frac{8k}{\rho c} \left(\frac{1}{1-D/D_f}\right) \ell n \left(1 + \frac{c\Delta T}{L}\right) t = \lambda_1 t \tag{11}$$

as reported by Godsave[2] for evaporation and burning in still air. However, for drops moving relative to the air stream, the assumption does not appear to be a valid one.

Considering the laminar boundary layer around solid spheres in motion, Tomotika[3] gives the following boundary layer equations:

$$v_1 = (1.5\,\theta - 0.36402\,\theta^3 + 0.024668\,\theta^5)v \tag{12}$$

and

$$\frac{v_1 \delta}{\nu} = C_1 \left(\frac{vD}{\nu}\right)^{1/2} \tag{13}$$

where C_1 is a dimensionless constant which depends on θ. Approximating Equation (12) by the first term and combining with Equation (13) yields the dynamic boundary layer thickness,

$$\delta = \frac{2}{3} \frac{C_1}{\sin \theta} \left(\frac{\nu D}{v}\right)^{1/2} . \tag{14}$$

Assuming the ratio between the thermal and dynamic boundary layer thicknesses can be expressed by

$$\frac{\delta_t}{\delta} = f_1 \,(N_{Pr})^{-1/3} \tag{15}$$

where f_1 is a constant, the thermal boundary layer thickness becomes,

$$\delta_t = \frac{D^{1/2}}{f(N_{Pr})^{1/3}\left(\frac{v}{\nu}\right)^{1/2}} \tag{16}$$

where

$$f = \frac{1}{\frac{2}{3} \frac{C_1}{\sin \theta} f_1} . \tag{17}$$

Substituting in

$$\frac{D}{D_f} = \frac{D}{D+2\,\delta_t} \tag{18}$$

and considering the case where the relative air velocity is a constant, the relationship between D_f and D is given by,

$$\frac{D}{D_f} = \frac{D^{1/2}}{D^{1/2} + C} \tag{19}$$

where C is given by Equation (3a).

Use of Equations (19) and (3a) permits the evaluation of the integral in Equation (10) leading to the evaporation Equation (3).

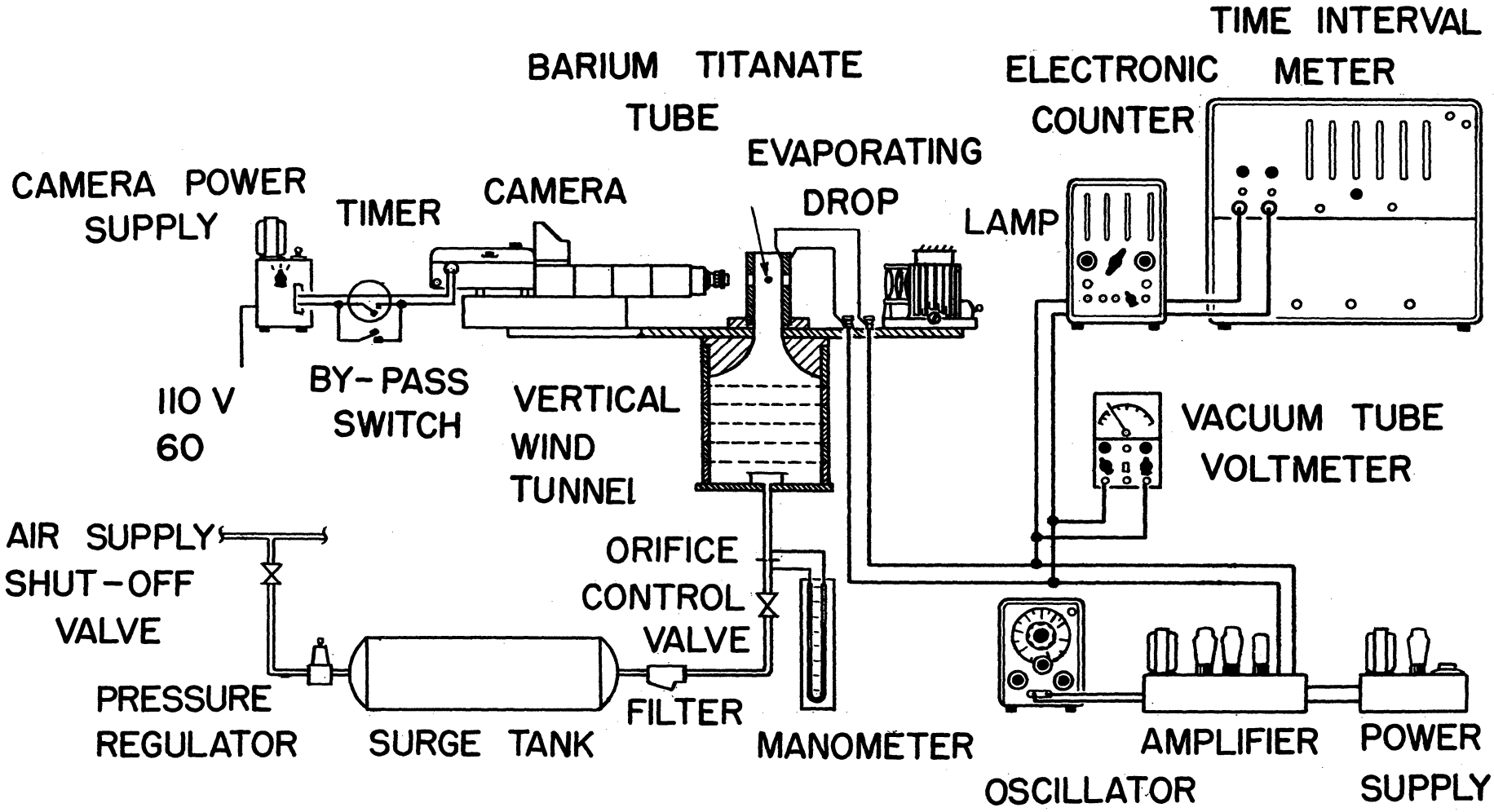

FIG 1. SCHEMATIC DIAGRAM OF EXPERIMENTAL EQUIPMENT

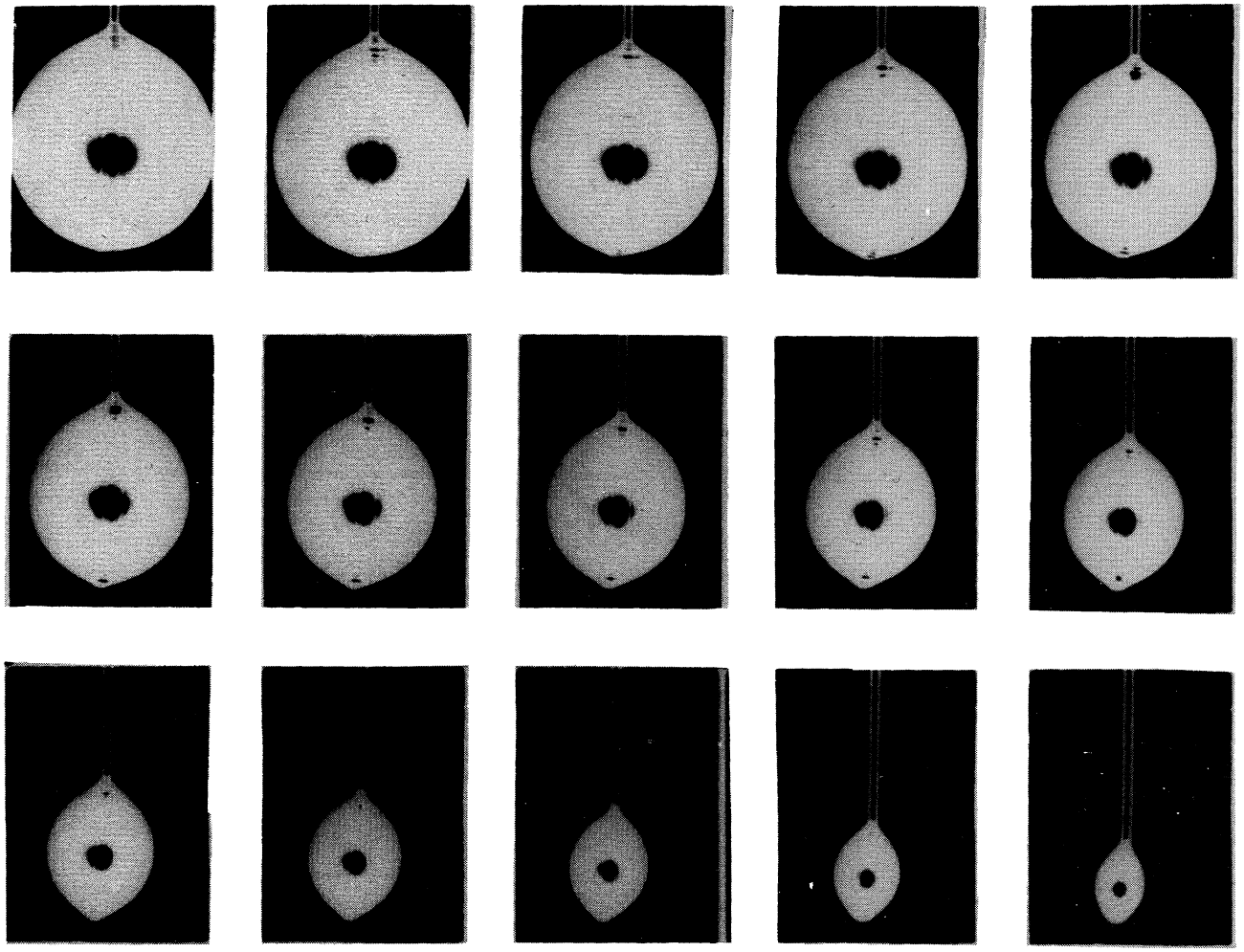

FIG. 2 EVAPORATING SUSPENDED DROP. D_o = 1112 MICRONS

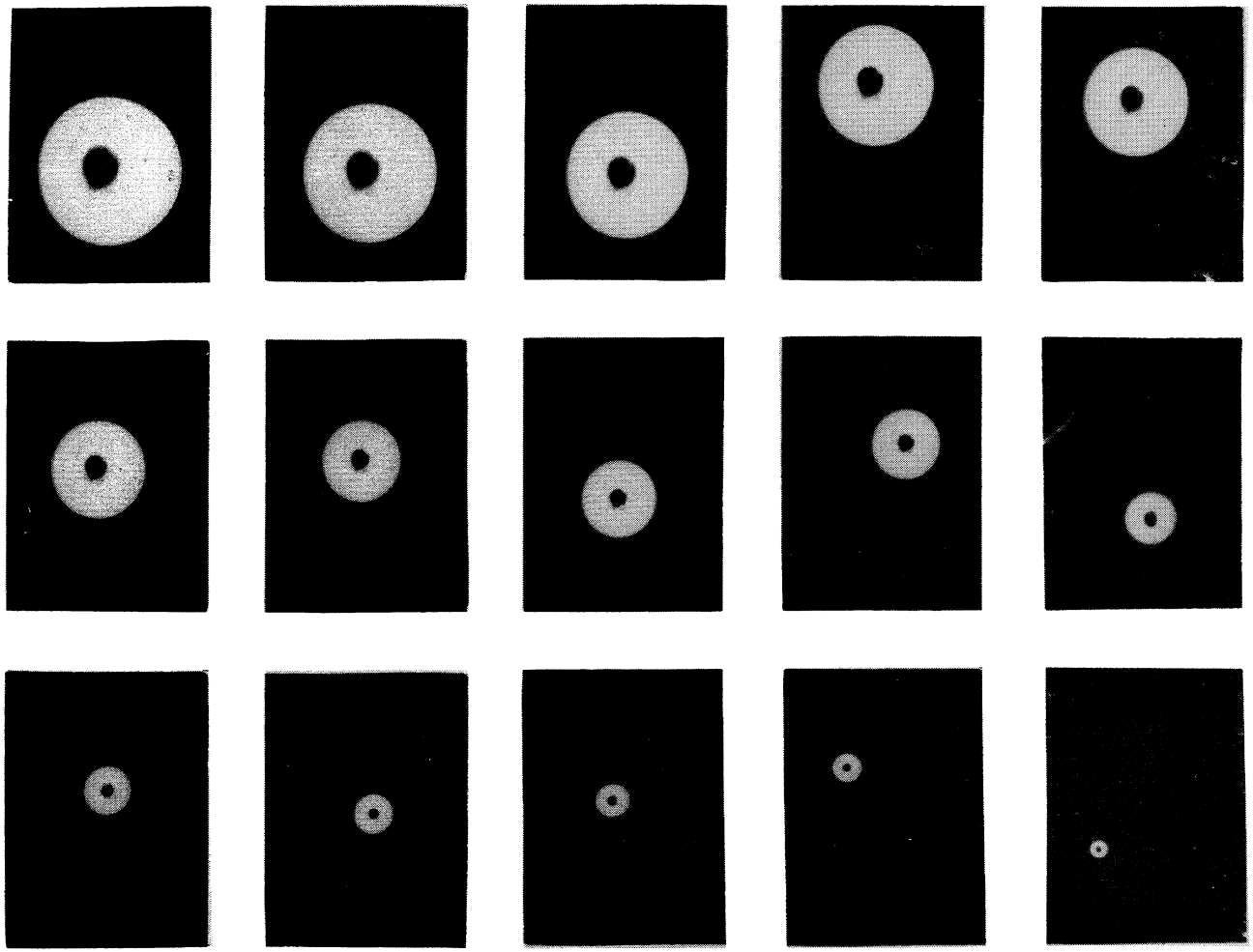

FIG. 3 EVAPORATING FREE DROP. D_o = 1178 MICRONS

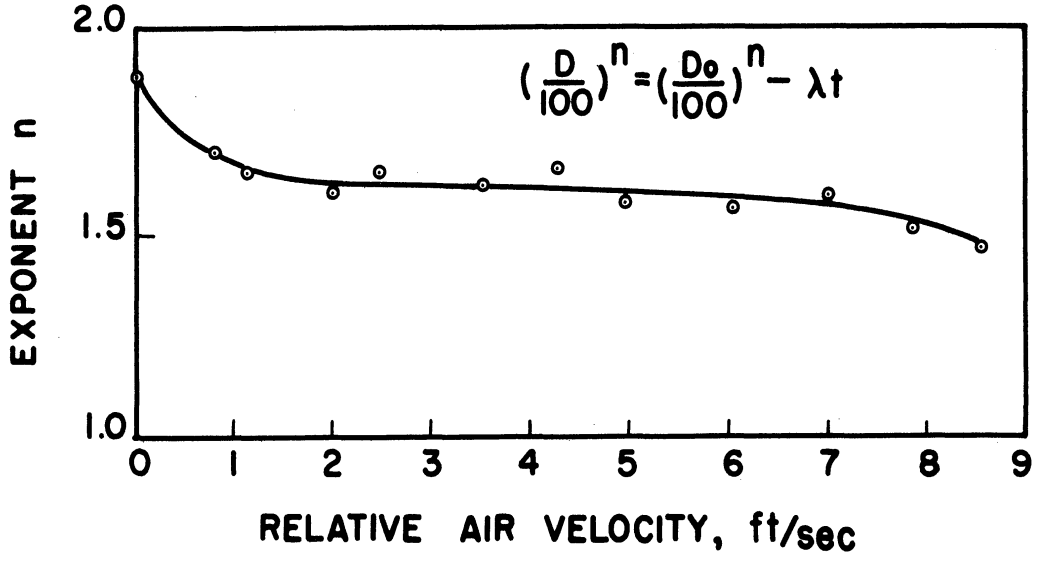

FIG. 4 VARIATION OF EXPONENT n WITH RELATIVE AIR VELOCITY.

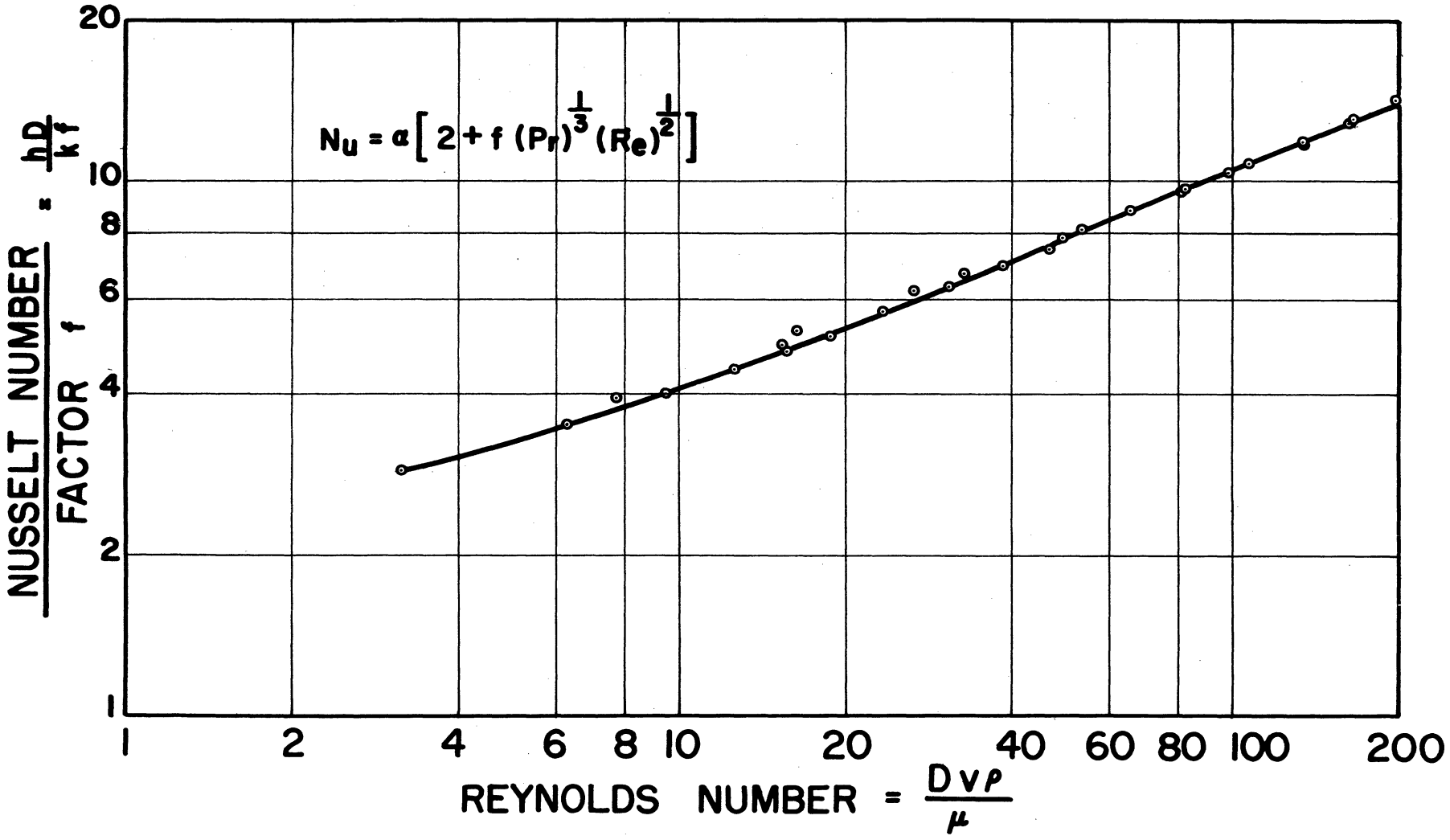

FIG.5 CORRELATION OF EVAPORATION DATA FOR SUSPENDED DROPS

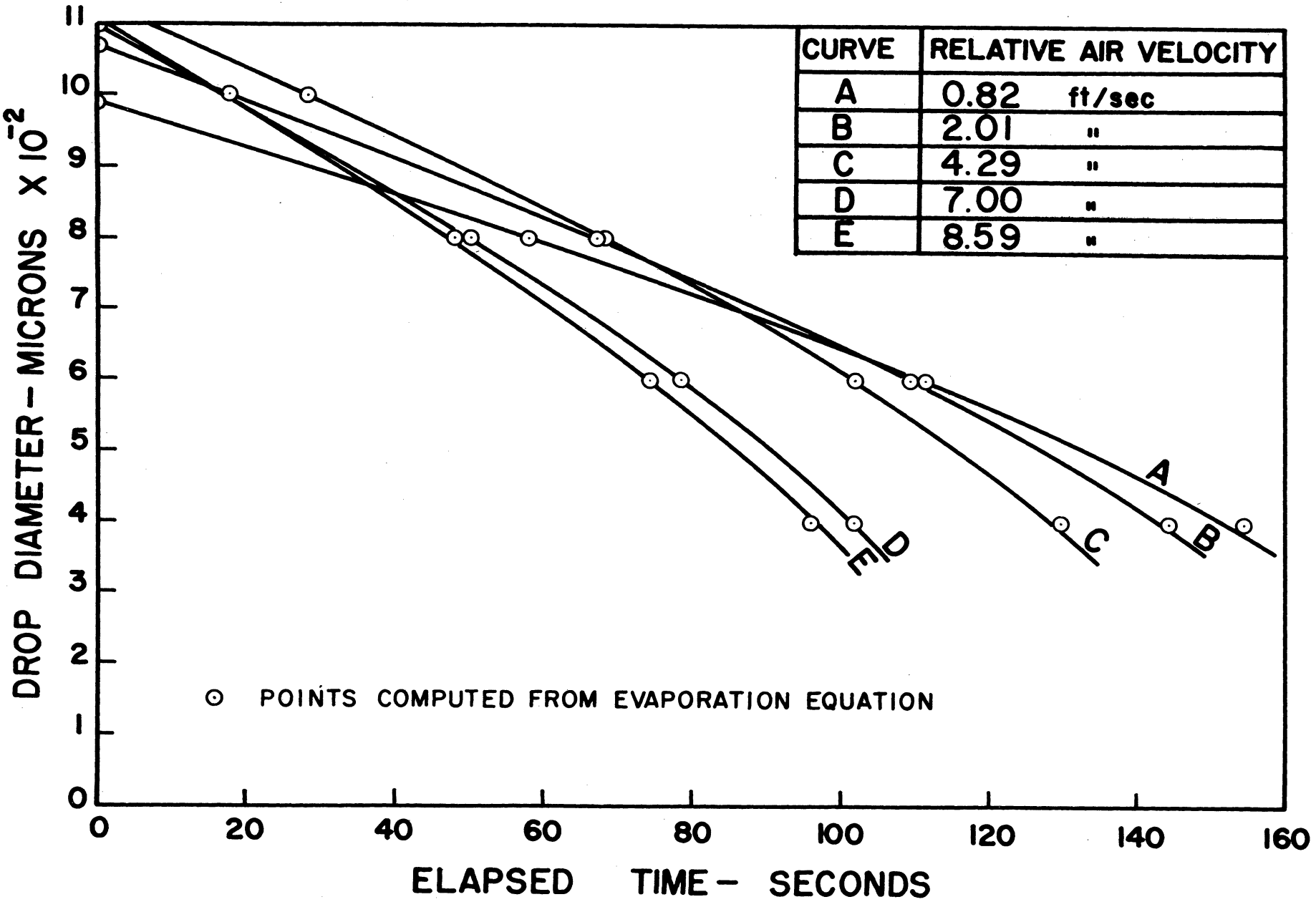

FIG. 6 EXPERIMENTAL CHECK OF EVAPORATION EQUATION.

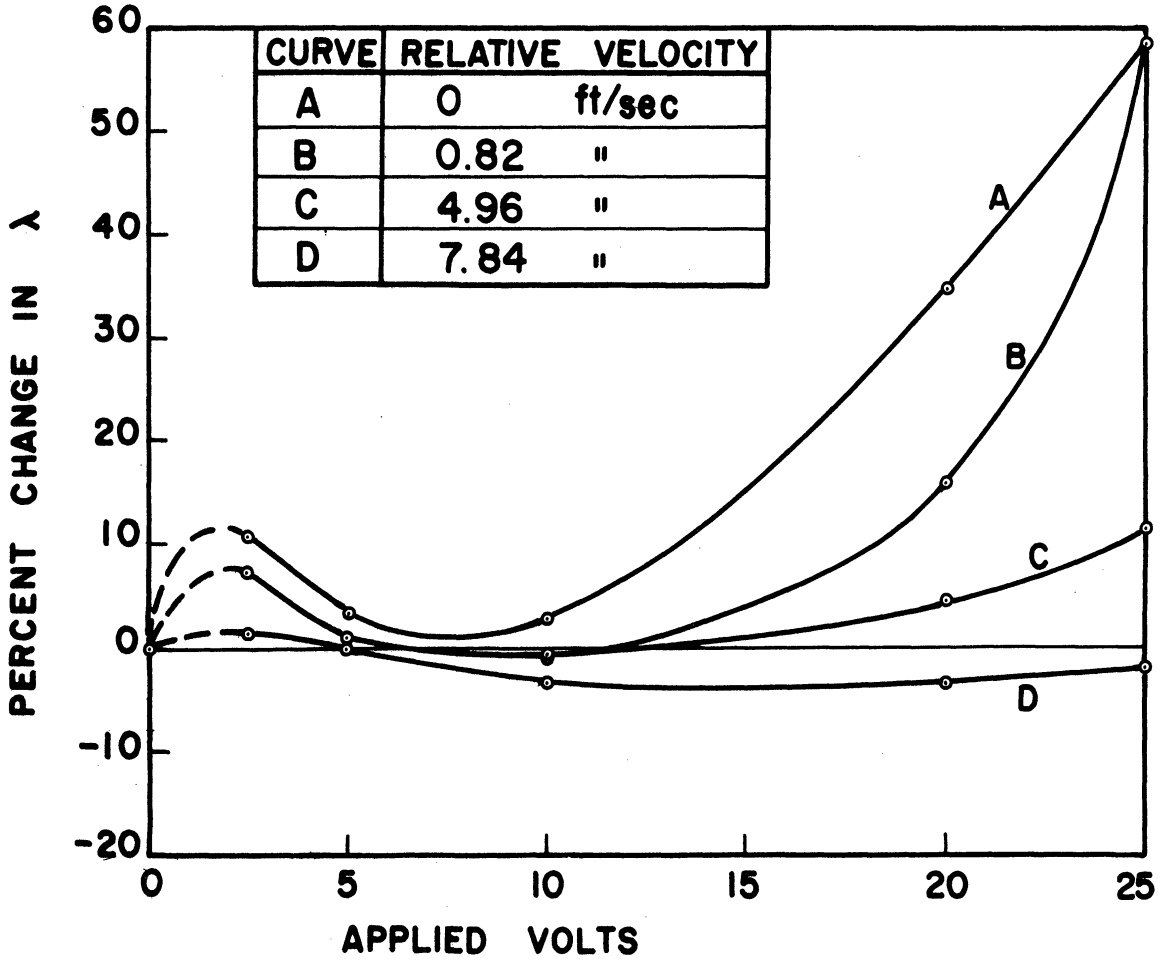

FIG. 7 PERCENT CHANGE IN λ DUE TO CHANGE IN FIELD INTENSITY AS MEASURED BY APPLIED VOLTS.

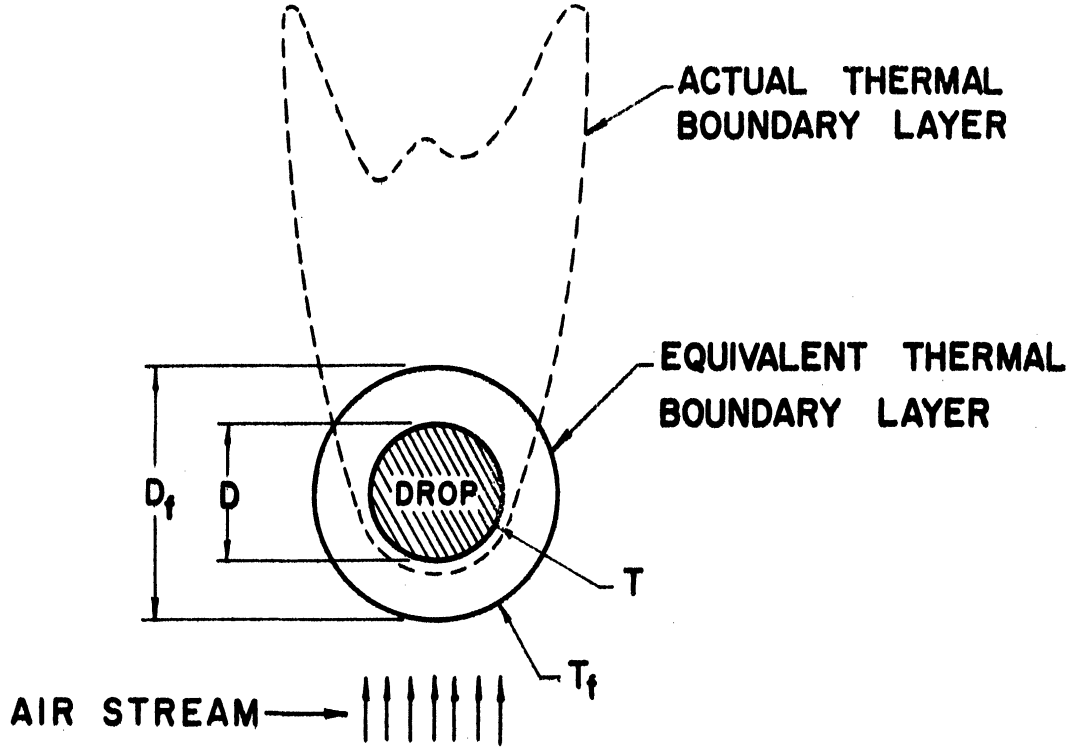

FIG. 8 MODEL OF EVAPORATING DROP.